International Journal of Nanomedicine

Dovepress
Taylor & Francis Group

Open Access Full Text Article

ORIGINAL RESEARCH

# Prenatal Delivery of HIF-1α siRNA Using Transferrin-Modified Lipid Nanoparticles Alleviates Hypoxia-Induced Neurodevelopmental Abnormalities via PTEN/PI3K/AKT Signaling

Feili Du, Yali Bai, Kexin Bai, Ting Yang, Jie Chen, Tingyu Li, Ying Dai

Department of Child Healthcare, Children's Hospital of Chongqing Medical University, National Clinical Research Center for Children and Adolescents' Health and Diseases, Ministry of Education Key Laboratory of Child Development and Disorders, Chongqing Key Laboratory of Child Neurodevelopment and Cognitive Disorders, Chongqing, 400014, People's Republic of China

Correspondence: Ying Dai, Email dai@hospital.cqmu.edu.cn



**Purpose:** Prenatal hypoxia is a major environmental risk factor for neurodevelopmental disorders, yet effective prenatal therapeutic strategies remain lacking. This study aimed to develop a transferrin-modified lipid nanoparticle platform for targeted delivery of HIF-1α siRNA to the fetal brain and to evaluate its therapeutic efficacy and molecular mechanisms.

**Methods:** Transferrin-modified lipid nanoparticles encapsulating HIF-1α siRNA were intravenously administered to pregnant rats prior to hypoxic exposure. Biodistribution, gene silencing efficiency, molecular signaling alterations, neuronal structural changes, and behavioral outcomes in offspring were systematically assessed.

**Results:** In this study, we developed a transferrin-modified lipid nanoparticle system for non-invasive, transplacental delivery of HIF-1α small interfering RNA to the fetal brain, achieving a siRNA encapsulation efficiency of 84.18% and a loading capacity of 2.5%. Systemic administration to pregnant rats prior to hypoxic exposure resulted in preferential accumulation of nanoparticles in fetal brain tissue and effective suppression of HIF-1α expression in the fetal hippocampus without overt effects on offspring survival, as evidenced by comparable offspring survival rates across all groups ($p > 0.05$). Prenatal hypoxia induced sustained elevation of HIF-1α protein ($p < 0.001$), impaired phosphatase and tensin homolog (PTEN) activity through increased phosphorylation ($p < 0.01$), aberrant activation of the PI3K/AKT signaling pathway ($p < 0.05$), and deficits in hippocampal neuronal structural plasticity, including reduced dendritic spine density ($p < 0.0001$) and dendritic complexity ($p < 0.0001$), accompanied by autism-like behaviors in offspring, including impaired social preference ($p < 0.01$), prolonged self-grooming ($p < 0.0001$), and increased marble-burying ($p < 0.001$). Prenatal HIF-1α silencing restored PTEN functional status, normalized PI3K/AKT signaling, improved dendritic architecture to levels comparable to controls ($p > 0.05$ vs control), and significantly ameliorated behavioral abnormalities (social preference and stereotyped behaviors, $p < 0.0001$). Mechanistic analyses revealed that although HIF-1α binds to the PTEN promoter (ChIP-qPCR, $p < 0.01$), prenatal hypoxia did not alter PTEN transcript or total protein levels ($p > 0.05$), indicating that HIF-1α primarily regulates PTEN function at the post-transcriptional level in vivo.

**Conclusion:** These findings identify a HIF-1α/PTEN/PI3K/AKT signaling axis as a key molecular pathway underlying hypoxia-associated neurodevelopmental impairment and demonstrate the feasibility of targeted prenatal gene modulation using transferrin-modified lipid nanoparticles. This work provides a nanomedicine-based framework linking environmental risk factors to early-life preventive strategies for neurodevelopmental disorders.

**Keywords:** transferrin-modified lipid nanoparticles, HIF-1α, PTEN, PI3K/AKT, prenatal hypoxia, fetal brain delivery, autism-like behaviors, RNA interference, prenatal gene delivery

## Introduction

Autism spectrum disorder (ASD), a neurodevelopmental condition characterized by impaired social reciprocity and restricted, repetitive behaviors, has become a serious public health concern affecting children's physical and mental health owing to its

https://doi.org/10.2147/IJN.S604443
Received: 21 February 2026
Accepted: 5 May 2026
Published: 13 May 2026

**Graphical Abstract**

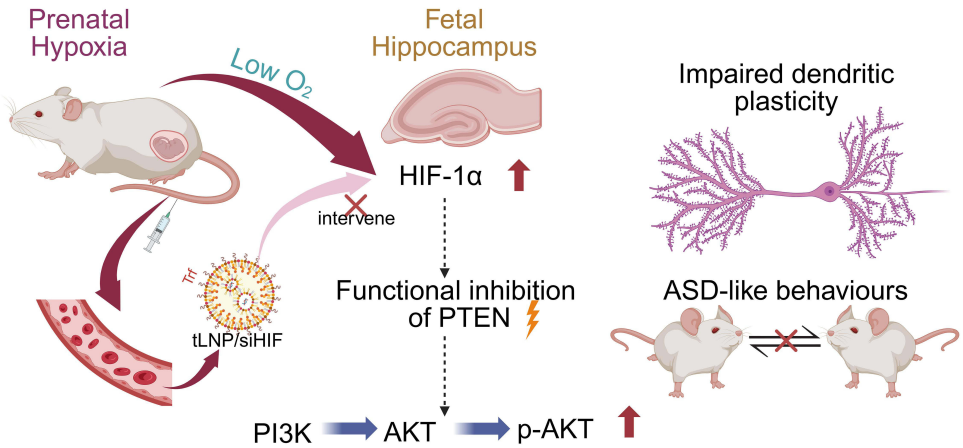


steadily rising prevalence.[1] According to the latest surveillance report from the CDC Autism and Developmental Disabilities Monitoring (ADDM) Network, the prevalence of ASD among U.S. children aged 8 years climbed to 32.2 per 1000 in 2022[2]—up from 27.6 per 1000 in 2020[3]—underscoring an accelerating diagnostic burden. The etiology of ASD is extremely complex, with adverse intrauterine environmental exposures attracting increasing attention.[4,5] Clinical epidemiological data demonstrate that prenatal hypoxia, such as fetal distress and placental insufficiency, significantly elevates the risk of ASD in offspring.[6,7] Oxygen deprivation in the critical period of embryonic development interferes with the processes of neuronal proliferation, migration, and synaptogenesis.[8] In spite of the fact that rodent models have demonstrated that prenatal hypoxia causes persistent social dysfunction and repetitive behavior in the offspring,[9,10] the early molecular events driving these pathological changes remain fully unelucidated.

Hypoxia-inducible factor-1α (HIF-1α) serves as a core transcriptional regulator in cellular responses to oxygen deprivation.[11] Previous findings from our group have established a strong correlation between prenatal hypoxia-induced HIF-1α enhancement and ASD-like behaviors in offspring, accompanied by alterations in PTEN-related signaling.[9,12] Moreover, we showed that interventions using either pharmacological approaches (the HIF-1α inhibitor PX-478) or genetic strategies (adeno-associated virus (AAV)-mediated HIF-1α silencing) effectively ameliorated social deficits and repetitive stereotypical behaviors in the offspring.[10,12] However, as both intervention strategies were implemented postnatally, they cannot sufficiently prove that HIF-1α is the key molecular mechanism for ASD-like behaviors following intrauterine hypoxia. Furthermore, a critical knowledge gap remains: whether aberrantly activated HIF-1α during late pregnancy, a vulnerable period for fetal neurodevelopment, directly interferes with PTEN transcription or post-translational modifications to trigger autism-like behaviors has not yet been confirmed.

To clarify whether HIF-1α is involved in this mechanism, targeted gene silencing using small interfering RNA (siRNA) represents an ideal strategy.[13,14] However, efficient prenatal genetic intervention faces substantial physiological barriers—the therapeutic agent must penetrate both the maternal placental barrier and the fetal blood-brain barrier (BBB).[15,16] In recent years, lipid nanoparticles (LNPs) have emerged as leading carriers for clinical translation due to their excellent nucleic acid protection capacity and biocompatibility.[14,17] Notably, transferrin receptors are highly expressed at the maternal-fetal interface (eg, placental trophoblast cells) and on fetal brain endothelial cells.[18,19] This physiological characteristic provides strong biological rationale for the development of nanomedicines capable of transplacental delivery with enriched fetal brain accumulation.

Against this backdrop, the present study designed and fabricated transferrin-modified lipid nanoparticles (tLNPs) for the targeted delivery of HIF-1α siRNA to the fetal brain during late gestation. The novelty of this study lies in two aspects: first, using the transferrin-modified lipid nanoparticles encapsulating HIF-1α siRNA (tLNP/siHIF) system as a "molecular scalpel", we confirmed, for the first time in vivo, that the HIF-1α/PTEN/PI3K/AKT cascade plays a core driving role in hypoxia-induced

neurodevelopmental abnormalities; second, we evaluated the feasibility of this nanomedical strategy as an early prenatal intervention. This work not only fills the mechanistic gap between environmental stress and neurodevelopmental disorders but also provides new translational insights for future nanotechnology-based maternal-fetal medical treatments.

# Materials and Methods

## Animals and Prenatal Hypoxia Model

### Animals

The SPF SD rats used in this experiment were purchased at the Experimental Animal Center of Chongqing Medical University [SPF, SCXK (Chongqing) 2018–0003], but then transferred to the Experimental Animal Facility of the Children's Hospital of Chongqing Medical University [SPF, SYXK (Chongqing) 2023–0011]. The animals were kept under controlled environment parameters, ie, the temperature was set to 21 °C, the relative humidity was set to 55–65%, and the lighting cycle was a standardized 12 hours of light and darkness. All the experimental work on animals was done in the Animal Research Center of the Children Hospital of Chongqing Medical University after the approval of the Experimental Animal Ethics Committee of the institution (Approval Number: CHCMU-IACUC20221122004). All animals were euthanized by intraperitoneal overdose of sodium pentobarbital (200 mg/kg) followed by cervical dislocation to ensure death, in accordance with the AVMA Guidelines for the Euthanasia of Animals (2020 edition).

### Model Building

A total of 8 male rats with body weights ranging from 220±20 g and 16 female rats were selected and housed overnight at a 1:2 pairing ratio. Pregnancy in female rats (marked as day 0.5 of gestation) was confirmed through vaginal plug examination, with sperm detection in vaginal smears conducted on the morning of day 2 before separate caging. The hypoxic chamber was prepared beforehand, containing bedding materials along with food and water supplies. Embryonic day 17 (E17) pregnant rats were placed in hypoxia chambers, injected with a mixed gas of nitrogen (90%) and oxygen (10%±0.5%), and monitored with a dedicated detector to maintain the oxygen concentration at 10%.[20] When the oxygen concentration reached 10%, rats were subjected to hypoxia for 6 hours.[9]

Pregnant SD rats were randomly assigned to four experimental groups. (1) Control group, in which pregnant dams were maintained under normoxic conditions throughout gestation; (2) Hypoxia group, in which pregnant dams were exposed to intrauterine hypoxia for 6 h on E17; (3) Hypoxia + tLNP group, in which pregnant dams received an intravenous injection of transferrin-modified blank lipid nanoparticle (tLNP) via the tail vein on E15, followed by hypoxic exposure for 6 h on E17; (4) Hypoxia + tLNP/siHIF group, in which pregnant dams were intravenously administered tLNP/siHIF via the tail vein on E15, followed by hypoxic exposure for 6 h on E17. To minimize potential sex-related variability, only male offspring aged 4–6 weeks were included in subsequent behavioral and molecular analyses. To reduce potential litter effects, offspring used for molecular, morphological, and behavioral analyses were selected from independent litters whenever possible, and litter origin was balanced across experimental groups. Investigators performing behavioral scoring and quantitative image analyses were blinded to group allocation.

## Synthesis and Characterization of Trf-LNP/siHIF-1α Nanoparticles

### siRNA Preparation

The HIF-1α small interfering RNA (siRNA) sequence of GCTCATCCAAGGAGCCTTA was obtained from Sangon Biotech (Shanghai) Company in Shanghai, China. Chemically modified siRNA targeting rat HIF-1α were synthesized commercially. For in vivo tracking, siRNA was labeled with Cy5.5.

### Lipid Nanoparticle Formulation

Lipid nanoparticles were prepared using a microfluidic mixing method. The final formulation was selected based on comprehensive optimization of particle size, PDI, encapsulation efficiency, and zeta potential.

The lipid components—DLin-MC3-DMA, DSPC, cholesterol, and DMG-PEG2000 (all supplied by Xi'an Ruixi Biological Technology Co., Ltd., Xi'an, China)—were combined at a molar ratio of 50:10:38.5:1.5 and dissolved in anhydrous ethanol to form the organic phase. For tLNP preparation, transferrin (Trf; Targetmol, Shanghai, China) was conjugated to the

distal end of the PEG-lipid. Briefly, Trf was dissolved in phosphate-buffered saline (PBS, pH 7.2–7.4). The carboxyl groups of Trf were then activated using 1-ethyl-3-(3-dimethylaminopropyl)carbodiimide (EDC; Macklin, Shanghai, China) and N-hydroxysuccinimide (NHS; Sigma-Aldrich, St. Louis, MO, USA) at room temperature (pH 5.0–7.5) to form an active ester intermediate. Subsequently, the activated Trf was added to the LNP suspension and incubated at room temperature under neutral conditions (pH 7.0–7.4) to facilitate covalent conjugation. Following conjugation, unconjugated Trf and excess EDC/NHS reagents were removed by gel permeation chromatography (GPC) to yield purified tLNP. For tLNP/siHIF preparation, HIF-1α siRNA was incorporated into the aqueous phase prior to mixing. The amine-to-phosphate (N/P) ratio was set at 6.

The aqueous phase and the organic phase were rapidly combined at a volumetric ratio of 3:1 using an INano™ L/L$^{+}$ microfluidic nanoprecipitation system (Micro & Nano Technology, China) at a total flow rate of 12 mL/min. The resulting nanoparticle suspension was incubated at room temperature for 10 minutes to allow complete self-assembly. Following assembly, the suspension was diluted ten-fold with RNase-free PBS (pH 7.4) and concentrated by ultrafiltration using 100 kDa molecular weight cut-off centrifugal filter units (Amicon Ultra, Merck Millipore). This process was repeated three times to reduce the residual ethanol concentration to below 0.0005% and to equilibrate the formulation to physiological pH (7.2–7.4). The final formulations were stored at 4°C until use.

## Nanoparticle Characterization

### Particle Size, PDI, and Zeta Potential

The hydrodynamic particle size, polydispersity index (PDI), and zeta potential of tLNP and tLNP/siHIF were measured using phase analysis light scattering (PALS).

### Encapsulation Efficiency and Loading Capacity

The encapsulation efficiency (EE) of HIF-1α siRNA was determined by measuring the absorbance of unencapsulated siRNA in the supernatant at 260 nm using UV-visible spectrophotometry. EE was calculated using the equation: EE (%) = [(m_total − m_free) / m_total] × 100%, where m_total represents the total amount of HIF-1α siRNA added during formulation and m_free denotes the amount of free siRNA remaining in the supernatant. The loading capacity (LC) was calculated as the ratio of the amount of encapsulated siRNA to the total weight of the nanoparticle formulation.

### Fluorescence Analysis

Successful encapsulation of Cy5.5-labeled siRNA was confirmed by fluorescence spectrophotometry. Fluorescence signals from tLNP/siHIF and control formulations were recorded and compared to verify siRNA incorporation.

### Morphological Characterization

The morphology of tLNP and tLNP/siHIF was examined by transmission electron microscopy (TEM). Samples were prepared by depositing a droplet of the nanoparticle suspension onto a carbon-coated copper grid, followed by negative staining and air-drying prior to imaging.

### Formulation Stability

Formulation stability was evaluated by monitoring changes in particle size over one week under two storage conditions: refrigerated temperature (4°C) and physiological temperature (37°C). Samples were measured at predetermined time points to assess colloidal stability during storage.

## Detection of Transferrin Modification by Dot Blot Analysis

To verify the surface modification of transferrin on LNP formulations, dot blot analysis was performed. Equal volumes (1 μL) of LNP, tLNP, and tLNP/siHIF suspensions were spotted onto polyvinylidene fluoride (PVDF) membranes (pre-activated with methanol for 1 minute) and allowed to air-dry at room temperature for 30–60 minutes to ensure complete sample fixation. Free transferrin (Trf) protein was included as a positive control, and unmodified LNP served as a negative control. Membranes were blocked with 5% non-fat dry milk in Tris-buffered saline containing 0.1% Tween-20 (TBS-T) for 1 hour at room temperature with gentle agitation. Membranes were then incubated overnight at 4°C with a primary anti-transferrin antibody (Zen-BioScience, Cat. No. P02787; 1:1000 dilution). After three washes with TBS-T (5 minutes each), membranes were incubated

with a horseradish peroxidase (HRP)-conjugated secondary antibody for 1 hour at room temperature. Protein signals were visualized using an enhanced chemiluminescence (ECL) detection system.

## In vivo Administration of LNPs

tLNP or tLNP/siHIF were injected into the tail vein of pregnant SD rats on gestational day 15 (E15). Prior to injection, pregnant dams were briefly anesthetized via inhalation of 2–3% isoflurane in oxygen using a nose cone, and maintained under 1.5–2% isoflurane for the duration of the procedure (approximately 3–5 minutes). Anesthesia was confirmed by loss of righting reflex and absence of response to toe pinch. 500 μL of tLNP or 500 μL of tLNP/siHIF (containing 50 μg of siRNA) was injected into the tail vein of each pregnant rat using an insulin syringe. The siRNA dose of 50 μg per animal was selected based on a previously established protocol for non-invasive transplacental gene delivery to the fetal brain using lipid-based nanoparticle systems,[21] and is consistent with reported effective doses for LNP-mediated siRNA silencing in rodent models.[22,23] Administration at E15 (48 hours prior to hypoxic exposure at E17) was designed to allow sufficient time for nanoparticle transplacental transfer, cellular uptake, endosomal escape, and RISC-mediated target mRNA degradation prior to the onset of hypoxic stress. This timing is consistent with the established kinetics of siRNA-mediated gene silencing, wherein maximal knockdown is typically achieved within 24–72 hours following intracellular delivery,[23,24] and with prior studies demonstrating that LNP-encapsulated nucleic acids can be detected in fetal brain tissue within 48 hours of maternal intravenous administration.[21]

## In vivo and ex vivo Fluorescence Imaging

### Fetal Imaging

At 48 hours following nanoparticle administration, fetal rats were harvested, and fluorescence signals derived from tLNP/siHIF were detected using a animal imaging instrument (IVIS Lumina III).

### Brain Slice Imaging

Paraffin sections of fetal brain (10 μm) were scanned for Cy5.5 fluorescence. The same sections were subsequently counterstained with DAPI to provide nuclear structural references, ensuring that Cy5.5 and DAPI signals presented in the merged images were acquired from identical tissue sections.

## Prenatal Toxicity and Offspring Survival Assessment

To assess potential maternal and fetal toxicity associated with nanoparticle administration, offspring survival was monitored at birth. The survival rate was calculated for each litter as the percentage of live pups relative to the total number of delivered pups. Each litter was treated as an independent biological replicate.

## Real-Time PCR Analysis of mRNA Expression

Hippocampal tissue samples were processed for total RNA isolation employing the Simply P Total RNA Extraction kit (Bio Flux, China). Isolated RNA was reverse-transcribed into complementary DNA (cDNA) using ABScript Neo RT Master Mix for qPCR with gDNA removal (Abclonal, China), according to the manufacturer's instructions. Quantitative analysis of mRNA expression was performed via real-time PCR with 2X Universal SYBR Green Fast qPCR Mix (Abclonal, China) (RK21203, Abclonal), utilizing cDNA as the template on a CFX96 Touch Real-time PCR detection instrument (BioRad). The comparative 2^-ΔΔCt approach was applied to determine relative mRNA expression levels, specific primer sequences employed in the amplification process are detailed in Table 1.

## Western Blotting

Using a commercial extraction kit (KGP250, KeyGen Biotech, China) determine the total protein levels in hippocampal tissue samples. The protein concentration of each lysate was quantified with a bicinchoninic acid (BCA) assay (KGPBCA, KeyGen Biotech). The samples were heated at high temperature for 10 minutes in 5× loading buffer (AIWB-0025, Affinibody). Subsequently, the proteins along with molecular weight markers (RM02949, Abclonal, China) were resolved through SDS-polyacrylamide gel electrophoresis (10% gel) and subsequently transferred onto

**Table 1** Primer Sequences for Quantitative Real-Time PCR

| Target Gene | | Sequence |
|---|---|---|
| HIF-1α | Forward | 5'-GCGAGAACGAGAAGAAAAATAGG-3' |
| | Reverse | 5'-GTTGTGGGGAAGTGGCAA-3' |
| PTEN | Forward | 5'-TGGATTCGACTTAGACTTGACCT-3' |
| | Reverse | 5'-GGTGGGTTATGGTCTTCAAAAGG-3' |
| β-actin | Forward | 5'-GGAGATTACTGCCCTGGCTCCTA-3' |
| | Reverse | 5'-GACTCATCGTACTCCTGCTTGCTG-3' |

PVDF membranes. The membranes were sectioned horizontally based on the marker positions, followed by a 10-minute blocking step using blocking solution (G2052, Servicebio, China). Membranes were incubated overnight at 4°C with primary antibodies against HIF-1α, PTEN, p-PTEN, AKT, and p-AKT at the indicated dilutions, followed by appropriate secondary antibodies. After three washes with PBST, the membranes were incubated for one hour at room temperature with appropriate secondary antibodies. The protein bands were stained sequentially with the help of an ECL detection kit (P10100, NCM Biotech) and quantitative analysis was performed on ImageJ software, where the loading control used to normalize the data was β-actin.

## Behavioral Assessments in Offspring

Behavioral tests were conducted at 4–6 weeks of age by investigators blinded to group allocation. Tests included:

### Three-Chamber Social Interaction Test

The three-chamber social interaction apparatus comprised three lateral compartments. Age- and sex-matched wild-type (WT) rats served as unfamiliar stimulus partners. Each of the side chambers contained a small cylindrical cage to accommodate either a novel toy or the unfamiliar rat. During the social approach test, the positions of the first unfamiliar rat (marked as S1) and the object were alternated between compartments to minimize potential side preference. Any-Maze tracking software was used to quantify the time spent in the proximity regions of S1 and the toy during a 10-minute observation period. Subsequently, the social novelty phase was conducted by introducing a second unfamiliar rat (marked as S2) into the apparatus while removing the inanimate object. The software also recorded exploration times in the S1 and S2 zones in this 10-minute interval. The apparatus was subjected to rigorous sanitization with 75% ethanol solution after every testing round to achieve hygiene standards and remove the scent cues.

### Marble Burying Test

Rats were placed into a testing box with 5cm deep Fresh bedding. Above the bedding, there were 24 green glass marbles evenly spaced placed. Testing rats were recorded for 20 min. The buried number were counted manually in a blind manner.

### Self-Grooming Test

The experimental setup consisted of a black opaque acrylic open-field chamber measuring $48\times48\times60cm^3$, where rats were positioned at the center and permitted unrestricted movement. A 5-minute video recording captured the animals' behavioral patterns. Grooming activities were operationally defined to include facial cleaning motions, head and ear scratching/rubbing actions, as well as complete body cleaning behaviors.

All equipment was cleaned with 75% ethanol between sessions.

## Golgi-Cox Staining

Hippocampal neuronal morphology was assessed using a modified Golgi-Cox staining protocol. Rat pups were euthanized by intraperitoneal injection of sodium pentobarbital (200 mg/kg), and whole brains were rapidly removed, briefly rinsed with distilled water, and immediately immersed in Golgi fixation solution (Servicebio, China). Offspring brains were impregnated for 2 weeks, sectioned at 60 μm, and digitized using a Pannoramic Scanner (3DHISTECH, Hungary).

Slides were placed on the scanner tray, and images were acquired in bright-field mode using the Pannoramic Scanner software. Dendritic spine density and Sholl analysis were performed on hippocampal pyramidal neurons following established protocols.[25]

## Dual-Luciferase Reporter Assay

The dual luciferase reporter assay was conducted following established procedures (Promega, Madison, USA). Based on the predicted binding sites of rat HIF-1α on the PTEN promoter identified by LASAGNA-Search (Table 2), PTEN promoter fragments carrying either intact or site-mutated regulatory elements were cloned into luciferase reporter constructs and introduced into HEK293T cells together with pcDNA3.1-HIF-1α or corresponding control plasmids. Following a 48-hour incubation period, cellular lysates were prepared and analyzed using the Dual-Luciferase® Reporter Assay System (Promega), with firefly luciferase signals being quantified and normalized against Renilla luciferase activity serving as the internal control.[26,27]

## Chromatin Immunoprecipitation (ChIP-qPCR)

ChIP experiments were conducted utilizing a commercially available ChIP assay kit (GeneCreate, Wuhan, China). Freshly isolated hippocampal specimens (0.2–0.5 g) underwent cross-linking treatment with 1% formaldehyde solution (final concentration) for 10 minutes through gentle flask inversion at ambient temperature, followed by quenching with 0.125 M glycine solution for 5 minutes. The samples were washed several times with phosphate-buffered saline (PBS) and stored at −80°C. Tissue disruption was done with a lysis buffer of 50 mM HEPES, 150 mM NaCl, 1 mM EDTA, 0.1% SDS, 0.1% sodium deoxycholate, and 1% Triton X-100 containing protease inhibitor cocktail and incubating the mixture at room temperature for 10 minutes. After centrifugation, the supernatant was decanted and the pellet was resuspended in the lysis buffer before sonication. The resulting fragmented chromatin was further incubated overnight with antibodies coupled to PierceTM Protein A/G Agarose Beads (Thermo Fisher Scientific, Inc). The next step was elution and removal of cross-links at 65°C overnight. The DNA extraction procedure was carried out by adding TE buffer (10 mM Tris-HCl, 1 mM EDTA) to the elution buffer and then treating successively with RNase (0.5 mg/mL) at 37 °C and proteinase K (0.3 mg/mL) at 51°C for one hour and then purifying the DNA. Immunoprecipitated chromatin fragments encompassing putative HIF-1α-responsive regions of the PTEN promoter were quantified by real-time PCR, with relative enrichment determined through comparative Ct analysis. The primer sequences used for the amplification of target genes are detailed in Table 3.

## Statistical Analysis

Data are presented as mean ± SEM. Statistical analyses were performed using GraphPad Prism 9. The experimental unit was defined according to each assay: independent litters were used for offspring survival analysis, animals derived from independent litters were used for in vivo molecular, morphological, and behavioral analyses, and independent transfections or independently prepared formulations were used for in vitro and nanoparticle characterization experiments. Normality and homogeneity of variance were assessed using the Shapiro–Wilk and Brown–Forsythe tests, respectively. Comparisons between two independent groups were performed using an unpaired two-tailed Student's *t*-test. Comparisons among multiple groups were performed using one-way ANOVA followed by Tukey's post hoc test. For datasets involving two factors or repeated measurements, including three-chamber behavioral tests, Sholl analysis, and formulation stability assays, two-way ANOVA or two-way repeated-measures ANOVA followed by post hoc multiple

**Table 2** Predicted Binding Site of Rat HIF-1α on the Promoter of PTEN by LASAGNA-Search

| Name | Start | Strand | Predicted Sequence |
|---|---|---|---|
| Pten-WT1 | 648 | + | GCACGTGC |
| Pten-WT2 | 1043 | + | GAACGTGC |

**Note**: "+" indicates the sense (forward) strand of the DNA sequence.


https://doi.org/10.2147/IJN.S604443

**Table 3** Primer Sequences for Chromatin Immunoprecipitation (ChIP)-qPCR Targeting the PTEN Promoter

| Target Gene | | Sequence |
|---|---|---|
| Pten | Forward1 | 5'-GGAACAGCTTGGGGACTCTC-3' |
| Pten | Reverse1 | 5'-CCCCTCTCTTCGGAGTCAGA-3' |
| Pten | Forward2 | 5'-AGCAGAGAGGGGTGGCG-3' |
| Pten | Reverse2 | 5'-CAGCTGAACCCCTCTCTTCG-3' |
| Pten | Forward3 | 5'-ACAAGCGAAAGGGAGGAA-3' |
| Pten | Reverse3 | 5'-CGGAGTCAGAGCGGAGAA-3' |
| Pten | Forward4 | 5'-CAGTAACCGGGTCCTCGAAC-3' |
| Pten | Reverse4 | 5'-GTCCACCGGATCACAGTCAG-3' |
| Pten | Forward5 | 5'-ACCGTCCCATACTCCACA-3' |
| Pten | Reverse5 | 5'-CACAGTCAGGCTCCATCT-3' |
| Pten | Forward6 | 5'-CGACCGTCCCATACTCCA-3' |
| Pten | Reverse6 | 5'-GTCAGGCTCCATCTTCTA-3' |

comparisons was applied as appropriate. A two-sided $P < 0.05$ was considered statistically significant. Exact sample sizes are indicated in the figure legends.

# Results

## Construction and Characterization of tLNP and tLNP/siHIF

tLNP and tLNP/siHIF were characterized to evaluate their physicochemical properties. As shown in Figure 1A, both formulations exhibited nanoscale particle sizes with narrow size distributions and low PDI values. Compared with tLNP, a slight increase in particle size and PDI was observed after siRNA loading, suggesting successful incorporation of siRNA into the lipid nanoparticle system. Zeta potential measurements demonstrated that both tLNP and tLNP/siHIF possessed positively charged surfaces (Figure 1B), which is attributable to the ionizable cationic lipid DLin-MC3-DMA undergoing protonation under the mildly acidic conditions used during formulation; although a slight difference in zeta potential was observed between tLNP and tLNP/siHIF, this difference did not reach statistical significance. UV-visible spectroscopy revealed absorbance profiles in the tLNP/siHIF formulation consistent with the expected spectral contributions of transferrin and Cy5.5-labeled siRNA, providing supporting evidence for surface modification and siRNA loading (Figure 1C). High-intensity Cy5.5 fluorescence signals were detected exclusively in the siRNA-containing lipid nanoparticles (LNPs) (Figure 1D), providing direct evidence of Cy5.5-siRNA encapsulation. Quantitative analysis indicated that the loading capacity of Cy5.5-HIF-1α-siRNA in tLNP/siHIF was 2.5%, with an encapsulation efficiency of 84.18%, demonstrating the high siRNA-loading capability of the transferrin-modified cationic lipid nanoparticle system. To further verify transferrin surface modification, dot blot analysis was performed; prominent transferrin-associated signals were detected on both tLNP and tLNP/siHIF, while unmodified LNPs lacked detectable labeling, confirming effective surface functionalization (Figure 1E). TEM imaging revealed that both tLNP and tLNP/siHIF adopted spherical morphologies with well-defined nanostructures, and no significant aggregation was observed after siRNA loading (Figure 1F). To assess formulation stability, particle size was monitored over 7 days under refrigerated (4°C) and physiological (37°C) conditions. Both tLNP and tLNP/siHIF maintained stable particle sizes with less than 10% variation throughout the observation period (Figure 1G), indicating favorable colloidal stability under both storage conditions.

## Efficient Fetal Brain-Targeted Delivery and in vivo Silencing of HIF-1α by tLNP/siHIF

In this study, tLNP/siHIF were administered via tail vein injection to pregnant rats on gestational day 15. On gestational day 17, Cy5.5 fluorescence signals from tLNP/siHIF in the fetus were tracked using a small animal in vivo imaging system (PE IVIS Lumina III). In comparison with the control group, significantly fluorescence signals were observed in the fetal brains of rats within the tLNP/siHIF group (Figure 2A). On day 17 of gestation, cesarean section was performed to obtain fetal rat brains for paraffin sectioning. Fluorescence scanning of the fetal rat brain sections revealed Cy5.5 red fluorescence (Figure 2B). These

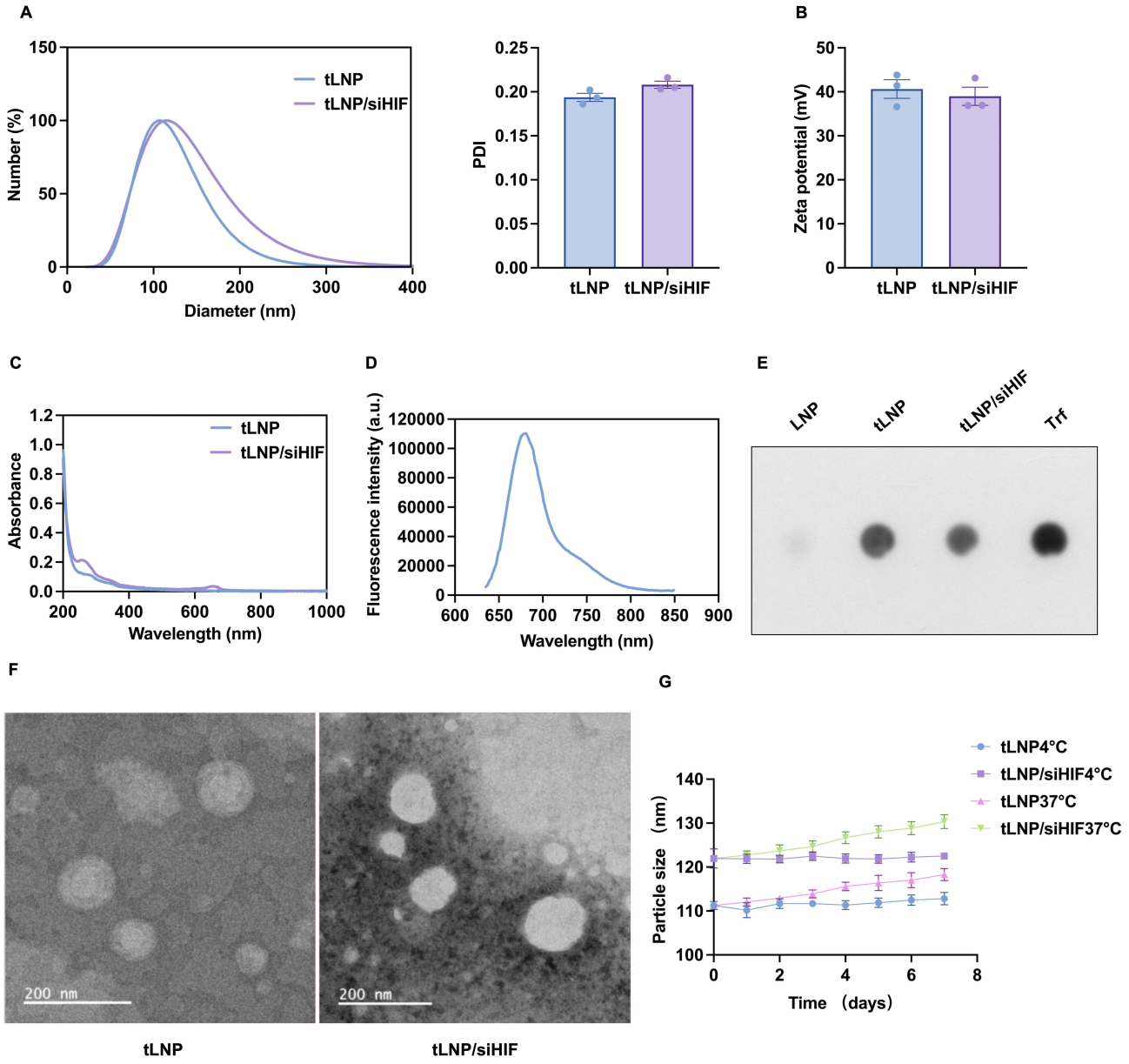


**Figure 1** Physicochemical characterization and colloidal stability of tLNP and tLNP/siHIF. (**A**) Hydrodynamic diameter distribution and PDI of tLNP and tLNP/siHIF measured by phase analysis of light scattering (PALS). (**B**) Zeta potential of tLNP and tLNP/siHIF. (**C**) UV-visible absorption spectra of tLNP and tLNP/siHIF. (**D**) Fluorescence emission spectrum of Cy5.5-labeled HIF-1α siRNA-loaded tLNP/siHIF, confirming successful siRNA encapsulation. (**E**) Dot blot analysis confirming transferrin surface modification of tLNP and tLNP/siHIF; unmodified LNP served as a negative control and free transferrin (Trf) as a positive control. (**F**) Transmission electron microscopy (TEM) images showing the spherical morphology of tLNP and tLNP/siHIF. Scale bar: 200 nm. (**G**) Colloidal stability of tLNP and tLNP/siHIF monitored over 7 days under refrigerated (4°C) and physiological (37°C) storage conditions. Both formulations maintained stable particle size with less than 10% variation throughout the observation period. Data are presented as mean ± SEM (n = 3).

findings suggest that tLNP/siHIF can traverse the placental barrier and accumulate in the fetal brain, although the contribution of free dye or degraded cargo to the detected fluorescence signal cannot be formally excluded.

To determine whether this delivery resulted in functional gene silencing, HIF-1α mRNA levels in fetal hippocampal tissue were assessed by quantitative PCR. Quantitative PCR revealed a pronounced reduction of HIF-1α transcripts following siRNA delivery (Figure 2C). Consistently, immunoblotting demonstrated elevated HIF-1α protein abundance in hypoxia-exposed offspring, which was markedly attenuated after tLNP/siHIF administration (Figure 2D). Collectively, these results indicate that tLNP-mediated siRNA delivery not only reaches the fetal brain but also effectively silences HIF-1α expression in vivo.

To evaluate whether prenatal administration of transferrin-modified lipid nanoparticles induced overt reproductive toxicity, offspring survival was assessed at birth. Across all experimental groups (n = 8 dams per group), the survival rate


https://doi.org/10.2147/IJN.S604443

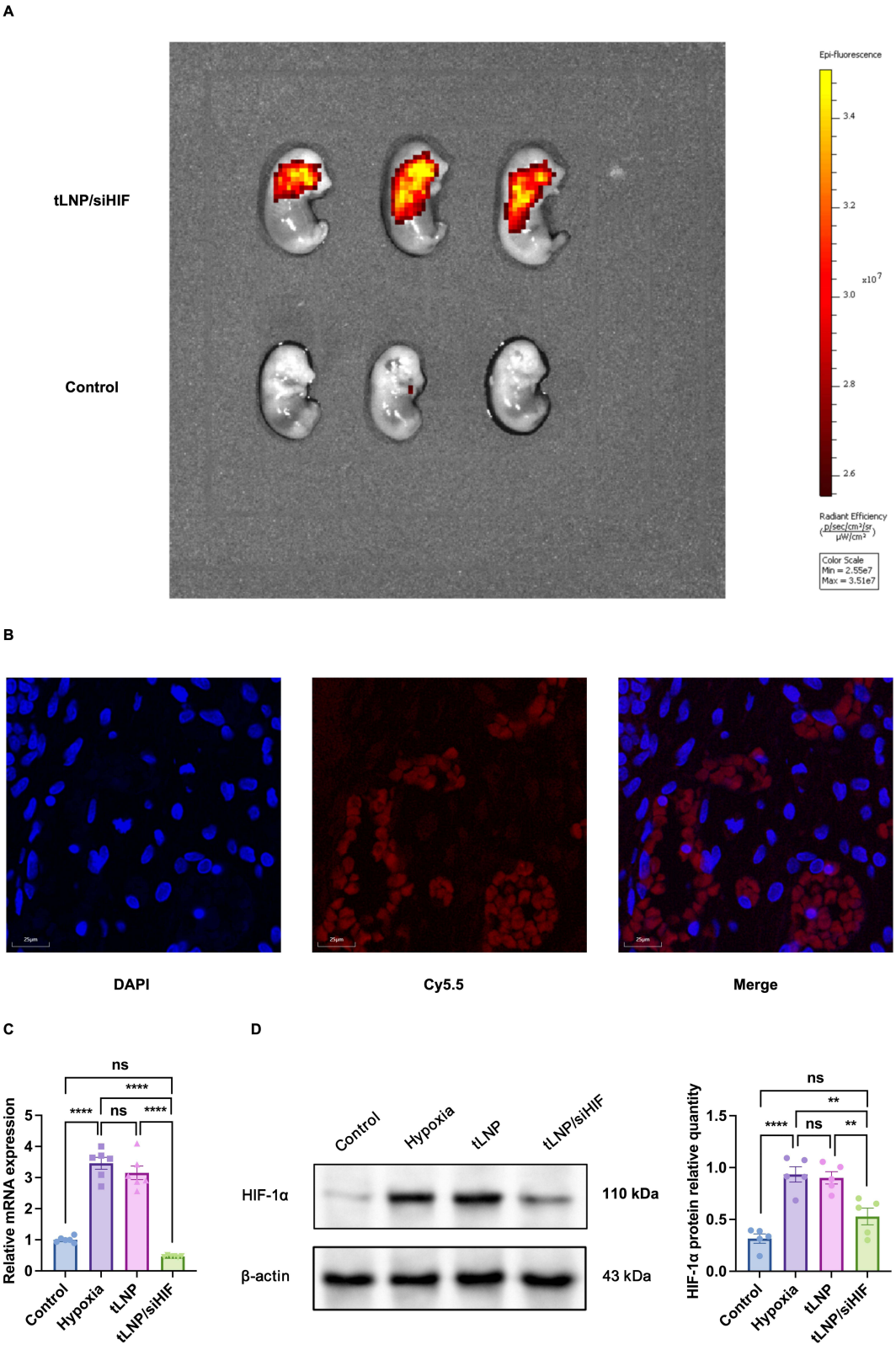


**Figure 2** tLNP/siHIF mediates placental crossing and effective silencing of HIF-1α in fetal brain. (**A**) Representative in vivo fluorescence images comparing Cy5.5 signal distribution between control and tLNP/siHIF groups (n = 3 fetuses from 3 independent litters). (**B**) Representative fluorescence images of fetal brain sections collected at E17 following maternal tail vein injection of tLNP/siHIF at E15, showing Cy5.5 fluorescence signals within the fetal brain; DAPI counterstaining was performed on the same tissue sections to provide nuclear reference. These results suggest that transferrin-modified lipid nanoparticles can traverse the placental barrier and accumulate in the fetal brain, though the contribution of free dye or degraded cargo cannot be formally excluded (n = 3 sections from 3 independent litters). (**C**) Quantitative PCR analysis of HIF-1α mRNA expression in fetal hippocampus (n = 6 animals from independent litters). (**D**) Representative immunoblots and quantitative analysis of fetal hippocampal HIF-1α protein expression (n = 5 animals from independent litters). Data are presented as mean ± SEM. **P < 0.01, ****P < 0.0001; ns, not significant.


https://doi.org/10.2147/IJN.S604443

remained high, with the majority of litters exhibiting 100% survival (Control: 133/134 pups, 99.3%; Hypoxia: 117/118 pups, 99.2%; tLNP: 121/121 pups, 100%; tLNP/siHIF: 121/121 pups, 100%). No statistically significant differences were observed among groups, indicating that prenatal nanoparticle-mediated HIF-1α silencing did not adversely affect neonatal viability (Supplementary Figure 1).

## Attenuation of Autism-Like Behavioral Abnormalities Following Prenatal Hypoxia through HIF-1α Suppression

Behavioral phenotyping was conducted in offspring rats at 4–6 weeks of age to determine how modulation of HIF-1α influences hypoxia-associated autism-like traits. Our prior research has demonstrated that exposure to hypoxic conditions during pregnancy leads to notable repetitive/stereotyped patterns and impaired social interactions in the offspring.[9] This hypoxia group thus served as the positive control for behavioral comparisons.

In the grooming test, the intrauterine hypoxia group exhibited significantly prolonged self-grooming duration, indicating increased stereotyped behaviors. HIF-1α siRNA intervention reduced grooming time to levels comparable with controls (Figure 3A). In the marble-burying test, the hypoxia group buried more marbles, reflecting heightened anxiety-like and stereotyped behaviors. The intervention group showed decreased marble burial similar to controls

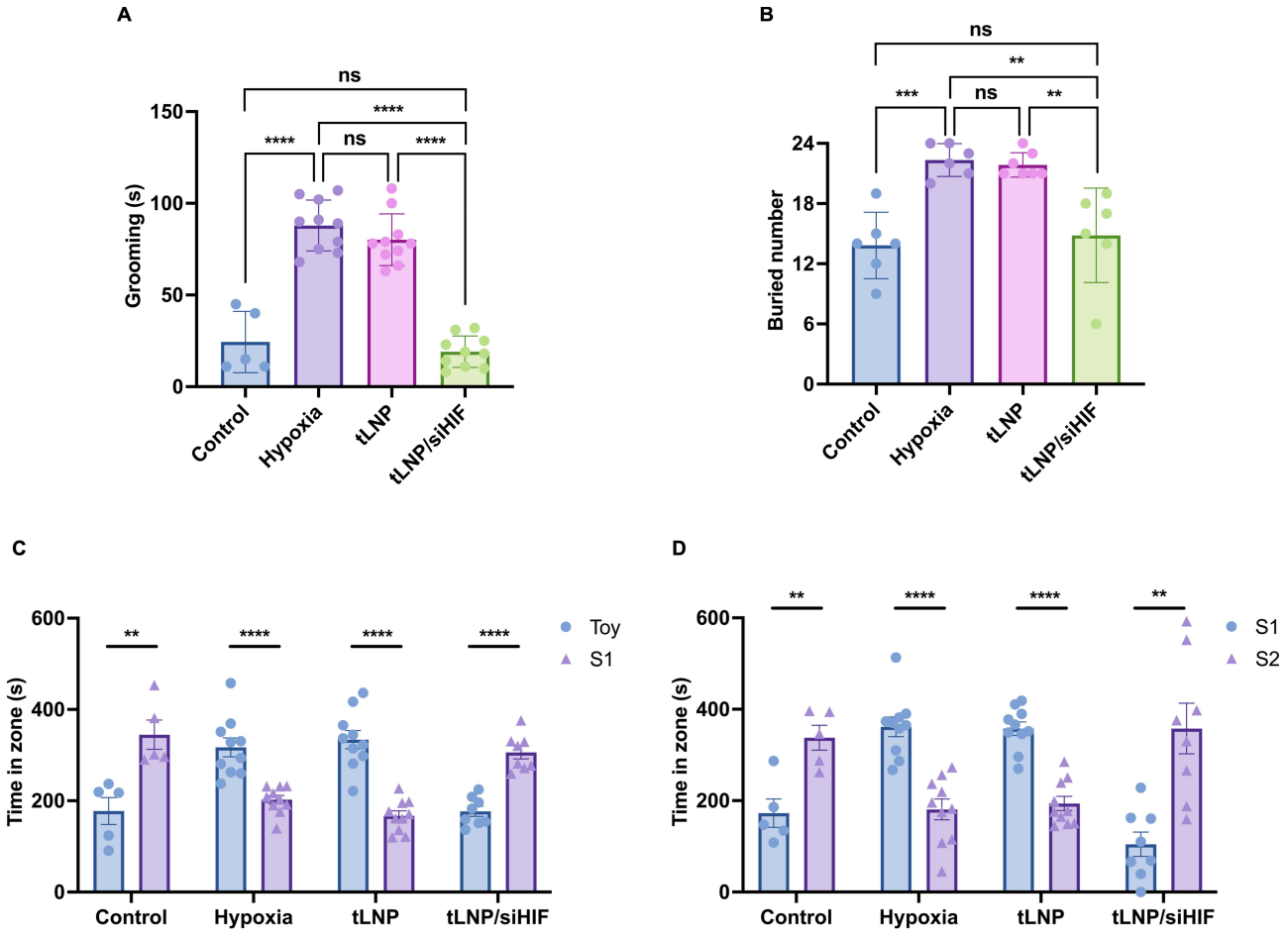


**Figure 3** Behavioral assessment of offspring at 4–6 weeks of age. (**A**) Self-grooming test showing total grooming duration per animal. (**B**) Marble burying test showing the number of marbles buried within 30 minutes. (**C**) Three-chamber social approach test showing time spent in the zone containing a stranger mouse (S1) versus an inanimate toy object (Toy) for each experimental group. A preference for S1 over Toy indicates intact social approach behavior. (**D**) Three-chamber social novelty test showing time spent in the zone containing a novel stranger mouse (S2) versus a familiar mouse (S1) for each experimental group. A preference for S2 over S1 indicates intact social novelty recognition. Hypoxia exposure induced significant increases in repetitive self-grooming and marble burying, and impaired both social approach and social novelty recognition in offspring, while tLNP/siHIF treatment restored these behaviors to levels comparable to the Control group. Data are presented as mean ± SEM (n = 5–10 animals per group, derived from 3 independent litters). **P < 0.01, ***P < 0.001, ****P < 0.0001; ns, not significant.


https://doi.org/10.2147/IJN.S604443

(Figure 3B). Social behavior was assessed using the three-chamber test. Prenatally hypoxic rats spent significantly more time in the toy-containing chamber (Figure 3C) and with S1-containing chamber (Figure 3D). The tLNP/siHIF group exhibited restored social preference, approaching control levels (Figure 3C and Figure 3D).

All three behavioral metrics confirmed that intrauterine hypoxia induces autism-like phenotypes. Specific inhibition of HIF-1α significantly ameliorated these behavioral abnormalities, supporting our hypothesis.

## Restoration of Hippocampal Neuronal Structural Plasticity Following HIF-1α Silencing

Golgi staining was performed on offspring hippocampal neurons to assess structural correlates of neural plasticity. The CA1 region in the prenatal hypoxia group exhibited a significant reduction in dendritic spine density (Figure 4A). Sholl

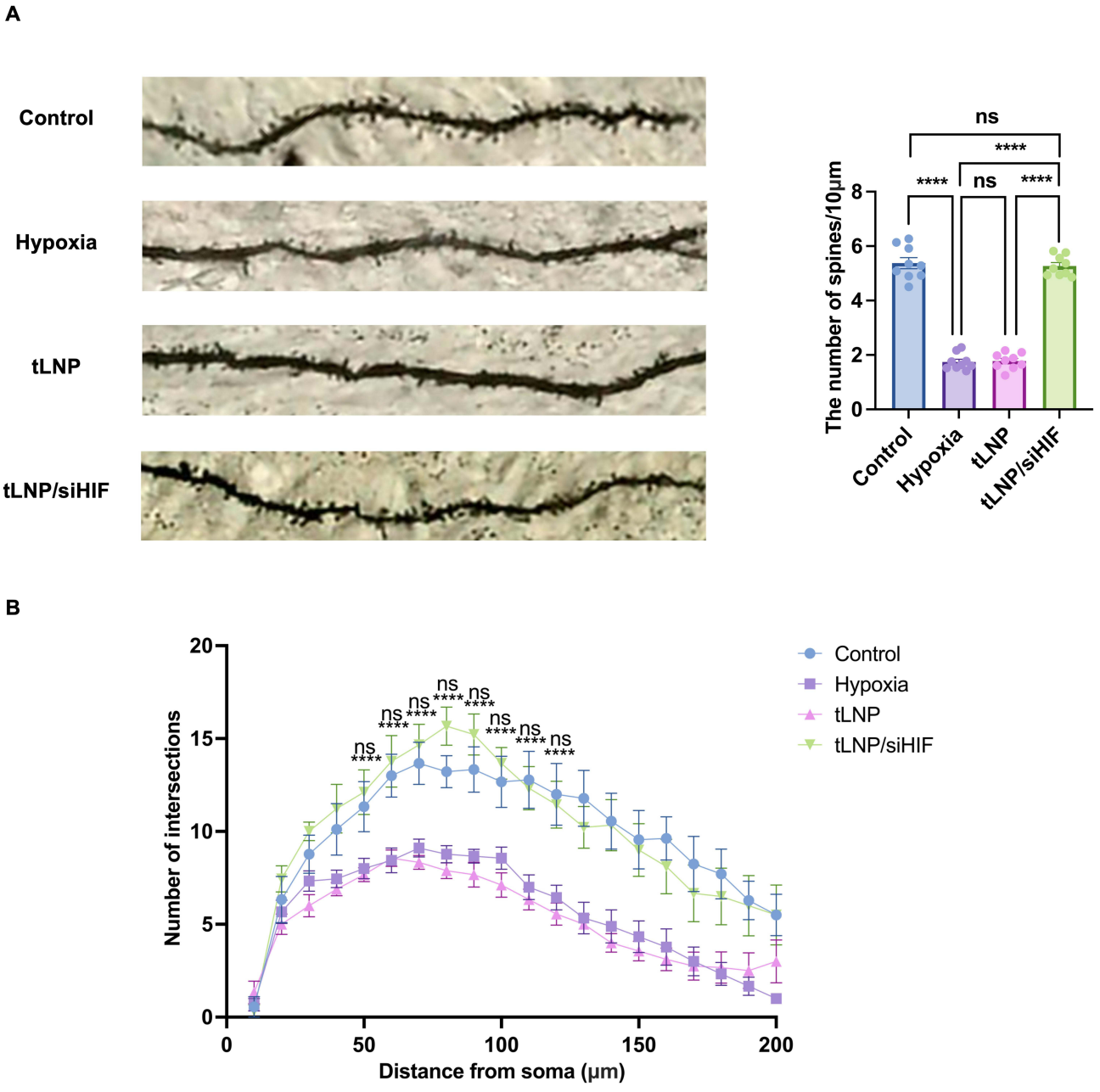


**Figure 4** Golgi staining of dendritic morphology in offspring neurons. (**A**) Representative Golgi-stained images of hippocampal pyramidal neuron dendrites and quantitative analysis of dendritic spine density in offspring rats from each group. (**B**) Sholl analysis showing dendritic complexity as the number of intersections at increasing distances from the soma. Data are presented as mean ± SEM (n = 3 animals per group, 1 animal per litter from 3 independent litters). ****P < 0.0001; ns, not significant. In Figure 4B, ****P < 0.0001 indicates significant differences between the Control and Hypoxia groups at each distance point; ns indicates no significant difference between the tLNP/siHIF and Control groups, demonstrating restoration of dendritic complexity following HIF-1α silencing.

analysis revealed a decreased number of intersections between dendrites and concentric circles (Figure 4B). These findings collectively indicate impaired neuronal complexity. However, in the intervention group, both metrics showed no significant difference compared to the control group, suggesting that HIF-1α siRNA effectively restores overall neuronal structural plasticity. These morphological results corroborate the behavioral and molecular data, confirming the neural injury induced by intrauterine hypoxia.

### Functional Modulation of PTEN via Promoter Engagement and Phosphorylation Mediated by HIF-1α, Leading to PI3K/AKT Signaling Activation

To elucidate the mechanisms by which HIF-1α influences PTEN and downstream PI3K/AKT signaling following prenatal hypoxia, PTEN regulation was systematically assessed at the mRNA, protein, and post-translational levels in offspring hippocampal tissue.

Immunoblotting revealed a pronounced elevation of HIF-1α protein abundance in the hippocampus following prenatal hypoxic exposure, while delivery of HIF-1α-targeting siRNA substantially normalized HIF-1α expression in offspring brains (Figure 5A). Prenatal hypoxia markedly increased PTEN phosphorylation, as reflected by an elevated p-PTEN/PTEN ratio (Figures 5B), while total PTEN protein levels remained unchanged (Figures 5G). Concurrently, enhanced AKT phosphorylation indicated activation of PI3K/AKT signaling, an effect that was effectively normalized by HIF-1α knockdown (Figure 5C).

To assess whether HIF-1α influences PTEN transcriptional control, dual-luciferase assays were performed using PTEN promoter fragments containing two predicted HIF-1α responsive elements. Dual-luciferase reporter assays demonstrated that increased HIF-1α activity significantly reduced the transcriptional activity of both wild-type PTEN promoter constructs (WT1 and WT2), supporting a direct interaction between HIF-1α and the PTEN promoter region (Figure 5D). Chromatin immunoprecipitation followed by quantitative PCR further demonstrated preferential occupancy of HIF-1α at specific regions of the PTEN promoter compared with IgG controls (Figure 5E). Despite detectable association of HIF-1α with the PTEN promoter, quantitative PCR analysis showed comparable PTEN mRNA levels across control, hypoxia, tLNP, and tLNP/siHIF groups (Figure 5F), suggesting that promoter binding does not translate into overt transcriptional suppression under hypoxic conditions.

Collectively, these results suggest that prenatal hypoxia-associated HIF-1α elevation primarily suppresses PTEN function via phosphorylation-dependent mechanisms, rather than by altering PTEN transcription or protein abundance, ultimately facilitating PI3K/AKT pathway activation during hippocampal development.

## Discussion

This study demonstrates that prenatal hypoxia exposure induces autism-like behaviors in offspring rats. This process is closely associated with coordinated molecular and structural alterations in the hippocampus, including sustained upregulation of HIF-1α, functional suppression of PTEN, aberrant activation of the PI3K/AKT signaling pathway, and impaired neuroplasticity. Critically, prenatal targeting of HIF-1α via transferrin-modified lipid nanoparticles reversed these molecular, structural, and behavioral deficits. These findings establish HIF-1α-dependent modulation of PTEN and PI3K/AKT signaling as an important molecular mechanism contributing to hypoxia-related neurodevelopmental impairment.

ASD is widely regarded as a multifactorial condition arising from the interplay of genetic susceptibility and environmental influences, although its precise etiological mechanisms remain unclear. While genetic contributions have been extensively investigated, studies addressing environmental risk factors are comparatively limited and face substantial methodological challenges.[28] In line with epidemiological findings, prenatal/perinatal hypoxic occurrences, such as fetal distress, low Apgar ratings, and birth asphyxia have been linked to the higher risk of ASD and neurodevelopmental severity.[29–31] We have also previously shown that rat prenatal hypoxia causes offspring to show ASD-like behaviors.[9] It is worth noting that the present study exclusively examined male offspring, a design choice intended to minimize hormonal variability and enhance statistical power. However, ASD exhibits a well-documented male predominance, with a male-to-female ratio of approximately 4:1, and emerging evidence suggests that sex-specific neurobiological mechanisms may differentially modulate vulnerability to prenatal hypoxic insults.[32,33] The extent to which the molecular and behavioral findings reported here apply to female

offspring therefore warrants investigation in future studies. Collectively, the present findings delineate a molecular framework linking prenatal hypoxic exposure to persistent alterations in neural development and behavioral outcomes.

Notably, hypoxic exposure during late gestation resulted in elevated hippocampal HIF-1α expression persisting into early adolescence (4–5 weeks of age),[9] indicating a sustained stress imprint rather than a transient adaptive response. Even though most of hippocampal neurogenesis is finished by half of gestation, considerable dendritogenesis and synaptogenesis takes place during the third trimester and into early postnatal life, suggesting that late gestation and early infancy are very important stages of hippocampal structural and functioning development.[34,35] Interference during this vulnerable developmental window may therefore impose long-lasting alterations in regulatory networks and signaling balance, ultimately maintaining elevated HIF-1α levels after birth.

HIF-1α is a master transcriptional regulator, which is activated by hypoxic condition and has been shown to coordinate cellular adaptation to oxygen starvation.[36] Although HIF-1α activation is essential for fetal adaptation to

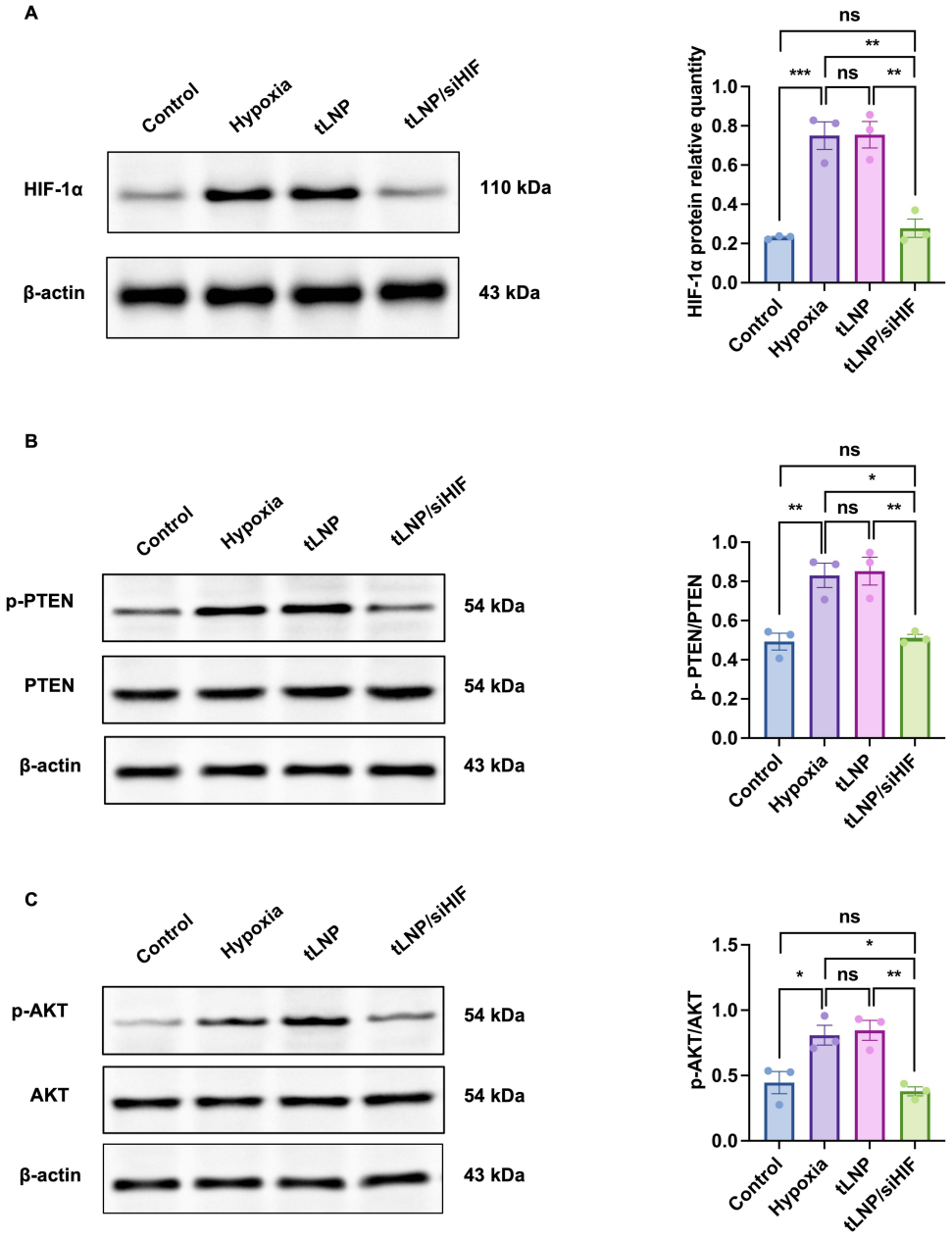


**Figure 5** Continued.

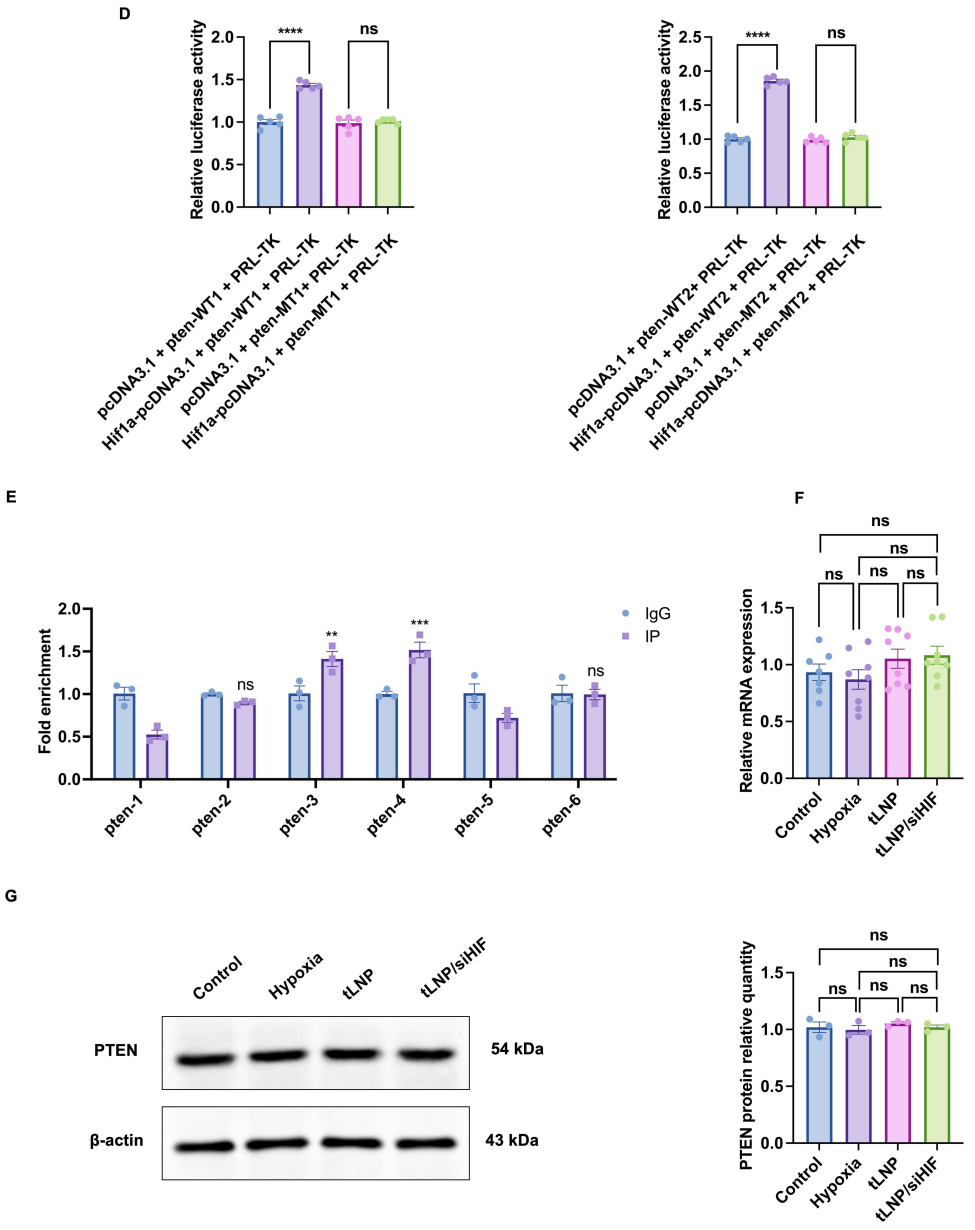


**Figure 5** Prenatal hypoxia enhances HIF-1α-dependent modulation of PTEN activity and PI3K/AKT signaling through promoter association and phosphorylation. (**A**) Representative immunoblot images and densitometric quantification of hippocampal HIF-1α protein levels in offspring rats (n = 3 animals from independent litters). (**B**) Representative immunoblots and quantification of PTEN phosphorylation levels expressed as the p-PTEN/PTEN ratio (n = 3 animals from independent litters) (**C**) Representative immunoblots and quantification of AKT activation expressed as the p-AKT/AKT ratio (n = 3 animals from independent litters). (**D**) Dual-luciferase reporter analysis assessing the impact of HIF-1α on PTEN promoter activity at two predicted binding regions (WT1 and WT2) (n = 5 independent transfection replicates per group). (**E**) ChIP-qPCR analysis demonstrating enrichment of HIF-1α at specific PTEN promoter regions compared with IgG controls (n = 3 animals from independent litters). (**F**) Quantitative PCR analysis of PTEN mRNA expression showing no significant differences among experimental groups (n = 7–8 animals from 3 independent litters). (**G**) Representative immunoblots and quantification of total PTEN protein levels normalized to β-actin (n = 3 animals from independent litters). Data are presented as mean ± SEM. *P < 0.05, **P < 0.01, ***P < 0.001, ****P < 0.0001; ns, not significant.

oxygen deprivation,[37,38] sustained or excessive signaling during critical periods of brain development may exert detrimental consequences. In parallel, hypoxia-exposed offspring displayed persistently elevated hippocampal HIF-1α levels accompanied by reduced dendritic spine density and simplified dendritic architecture, features commonly linked to ASD-related neuropathology.[39] Collectively, these observations suggest that targeting HIF-1α may hold therapeutic potential for mitigating hypoxia-associated neurodevelopmental abnormalities. Previous work from our group demonstrated that postnatal intracerebroventricular delivery of HIF-1α-modulating viral vectors mitigated behavioral and


https://doi.org/10.2147/IJN.S604443

neurodevelopmental deficits induced by prenatal hypoxia.[12] Nevertheless, effective in utero gene-specific manipulation of the fetal brain remains technically challenging, and experimental evidence directly linking HIF-1α to prenatal hypoxia-induced autism-related behaviors has been limited. Fetal gene delivery through yolk sac vein injection of various vectors has been accomplished in several studies;[40,41] but these methods necessitate invasive fetal surgery.[42] The application of these strategies in humans is severely limited due to potential risks to maternal health and fetal development, including infection, increased maternal morbidity, preterm labor, and fetal loss.[43] A methodological consideration warrants acknowledgment regarding the use of isoflurane anesthesia during intravenous administration. Isoflurane is known to transiently modulate placental vascular tone and may alter uteroplacental blood flow,[44,45] raising the question of whether enhanced fetal brain accumulation of tLNPs could partly reflect anesthesia-induced changes in placental permeability rather than exclusively transferrin receptor-mediated active targeting. While we cannot formally exclude this possibility in the absence of a dedicated pharmacokinetic comparison under awake versus anesthetized conditions, several lines of evidence support a receptor-mediated contribution: (1) the Cy5.5 signal was specifically detected in fetal brain tissue rather than uniformly distributed across all fetal organs (Figure 2A); (2) transferrin receptor expression is well-documented to be enriched at the maternal-fetal interface and fetal brain endothelium;[18,19,46] and (3) prior studies using transferrin receptor-targeted liposomal systems have demonstrated that receptor-mediated transplacental delivery and preferential fetal brain accumulation are achievable following maternal intravenous administration.[21] Nevertheless, future studies employing non-anesthetized delivery paradigms or direct comparison with untargeted LNP controls will be necessary to definitively establish the receptor-specificity of this delivery system. Transferrin receptors are abundantly expressed at the maternal-fetal interface and within the fetal blood-brain barrier, supporting their suitability for mediating targeted delivery to the developing brain.[47,48] Previous studies have demonstrated that transferrin receptor-targeted liposomal systems can facilitate non-invasive delivery of genetic material to the fetal brain.[21] Building on this delivery strategy, we applied transferrin receptor–targeted lipid nanoparticles to silence HIF-1α prior to hypoxic exposure, directly testing its causal role in prenatal hypoxia-induced autism-like phenotypes. Most importantly, this strategy provides proof-of-concept evidence for a potential preventive intervention in high-risk hypoxic pregnancies, offering a translationally relevant and non-invasive approach to early neurodevelopmental protection.

The safety profile of prenatal siRNA delivery via tLNPs merits careful consideration. In the present study, formal toxicological assessments of maternal hepatic and splenic function were not performed, and the potential for maternal HIF-1α silencing to indirectly compromise gestational homeostasis was not systematically evaluated. This represents a recognized limitation, as HIF-1α is an essential transcription factor for embryonic survival and normal organogenesis;[49] its systemic suppression during pregnancy could theoretically perturb placental angiogenesis, erythropoiesis, and oxygen-sensing mechanisms critical to fetal development. The consistently high offspring survival rates observed across all experimental groups provide indirect reassurance against gross developmental toxicity, and no overt signs of maternal distress were recorded during the study period. However, survival rate alone is an insensitive endpoint for detecting subtle teratogenic or organ-specific effects. Comprehensive maternal safety assessments—including hepatic enzyme panels, splenic histology, placental morphometry, and evaluation of non-CNS fetal organ development—will be essential before this approach can be considered for translational development. Future studies should also incorporate dose-escalation designs and extended postnatal follow-up to characterize the full safety window of prenatal tLNP administration. These considerations underscore the importance of treating the present findings as proof-of-concept mechanistic evidence rather than a clinically optimized intervention.

The PI3K/AKT pathway is a critical regulator of neural development, influencing neuronal survival, neurite extension, and synaptic function.[50] We found that elevated HIF-1α levels were accompanied by enhanced AKT phosphorylation, indicating functional engagement of the PI3K/AKT signaling cascade. Considering PTEN as a negative regulator of PI3K/AKT pathway and its association with ASD susceptibility,[51,52] these observations raise the possibility that PTEN function may be influenced by HIF-1α activity. To further delineate the molecular basis of HIF-1α-mediated PTEN regulation, dual-luciferase reporter assays and chromatin immunoprecipitation were performed, confirming direct HIF-1α association with the PTEN promoter. These data suggest that HIF-1α engagement contributes to altered PTEN signaling and downstream PI3K/AKT pathway activation under hypoxic conditions. Though reporter assays demonstrated direct interaction between HIF-1α and the PTEN promoter, neither PTEN transcript abundance nor total protein levels were

detectably altered in the hippocampus following prenatal hypoxic exposure. This dissociation suggests that, in vivo, HIF-1α predominantly modulates PTEN activity through post-translational mechanisms, particularly phosphorylation-dependent functional regulation, rather than sustained transcriptional suppression. This apparent discrepancy between in vitro transcriptional evidence and in vivo mRNA stability is not without precedent in the literature. PTEN protein activity is subject to extensive post-translational regulation, including phosphorylation at Ser380/Thr382/Thr383 residues by casein kinase 2 (CK2) and other kinases, ubiquitination-mediated proteasomal degradation, and oxidative inactivation —all of which can be modulated by hypoxic signaling independently of transcriptional output.[53,54] It is therefore plausible that HIF-1α binding to the PTEN promoter, as confirmed by ChIP-qPCR, represents a priming or sensitization mechanism that becomes functionally dominant under conditions of sustained or severe hypoxia, while the predominant acute regulatory effect in our model operates at the post-translational level. The normalization of PTEN phosphorylation status following HIF-1α silencing (Figure 5B) is consistent with this interpretation and provides functional evidence that HIF-1α contributes to PTEN dysregulation through mechanisms beyond transcriptional repression alone. Such context-dependent control is consistent with the notion that PTEN expression remains relatively stable during critical periods of brain development, favoring dynamic regulation of signaling activity over changes in gene abundance. Notably, prenatal HIF-1α silencing effectively normalized PTEN signaling (Figure 5B), attenuated PI3K/AKT overactivation (Figure 5C), improved hippocampal dendritic architecture (Figure 4), and alleviated autism-like behavioral deficits in offspring (Figure 3). These results indicate that HIF-1α is a key upstream regulator that synthesizes a hypoxic stress signal into long-term neurodevelopmental effects. Regarding the rationale for employing siRNA-mediated gene silencing in this context: although HIF-1α regulation of PTEN in vivo appears to operate predominantly at the post-translational level, reducing HIF-1α protein abundance through siRNA knockdown effectively diminishes the upstream hypoxic signal that drives these post-translational modifications. This approach therefore targets the root cause of the signaling dysregulation rather than its downstream manifestations, and the behavioral and molecular rescue observed following tLNP/siHIF treatment provides functional validation of this strategy. The use of siRNA also offers practical advantages over small-molecule inhibitors in terms of target specificity, particularly given the pleiotropic roles of HIF-1α in normal physiology.

The current study has a number of limitations that should be acknowledged. First, although the rat model captures key features relevant to ASD, the 4:1 male-to-female prevalence ratio characteristic of clinical populations was not systematically explored. Sex-specific differences in vulnerability to prenatal hypoxia or in the response to tLNP-mediated intervention remain to be characterized. Second, the present study focused exclusively on the hippocampus. However, ASD-related neuropathology also involves the prefrontal cortex, amygdala, and cerebellum.[55] Whether prenatal hypoxia induces analogous HIF-1α-dependent molecular alterations in these regions, and whether tLNP-mediated silencing exerts comparable rescue effects beyond the hippocampus, remains to be determined. Third, several aspects of the formulation require further characterization. Despite the favorable properties of lipid nanoparticles,[56,57] their in vivo performance can be constrained by preferential accumulation in reticuloendothelial organs.[58] Furthermore, the stability of tLNP/siHIF complexes in maternal serum and their in vitro siRNA release kinetics under physiologically relevant conditions were not directly assessed. Advanced physicochemical characterizations, including FTIR and DSC, were also not performed. These analyses are necessary to provide direct evidence of lipid–siRNA interactions, confirm transferrin conjugation integrity, and fully characterize the delivery system's in vivo pharmacokinetic behavior, and will be incorporated in future optimization work. Fourth, encapsulation efficiency in the present study was determined by UV-visible spectrophotometry at 260 nm, which may be subject to potential spectral interference from lipid components; future studies should incorporate fluorescence-based quantification methods, such as the RiboGreen assay, to provide more precise determination. Fifth, the biodistribution analysis relied on Cy5.5-labeled siRNA without the inclusion of a free dye control or a parallel group receiving non-functionalized LNPs. The absence of these controls limits our ability to unambiguously attribute the detected fluorescence signal to intact nanoparticle-encapsulated siRNA and to formally confirm that fetal brain accumulation reflects transferrin receptor-mediated active targeting rather than passive extravasation. Sixth, although all groups receiving intravenous administration underwent identical handling, the potential contribution of injection-related stress to behavioral outcomes cannot be entirely excluded and represents a confounding variable that future studies should address through the inclusion of non-injected naïve controls. Finally, comprehensive toxicological evaluation—including maternal hepatic and splenic health, placental integrity, long-term

neurodevelopmental follow-up, and multi-organ histopathological analysis—will be essential to establish the preclinical safety profile required for translational advancement.

## Conclusion

In conclusion, this study demonstrates that prenatal hypoxic exposure induces persistent neurodevelopmental abnormalities in offspring, including autism-like behavioral phenotypes, impaired hippocampal neuronal structural plasticity, and dysregulation of the HIF-1α/PTEN/PI3K/AKT signaling pathway. Using transferrin-modified lipid nanoparticles as a non-invasive maternal-fetal delivery platform, we achieved fetal brain accumulation of HIF-1α siRNA and effective suppression of HIF-1α expression during late gestation. Importantly, prenatal HIF-1α silencing restored PTEN functional status, attenuated aberrant PI3K/AKT activation, improved dendritic spine density and dendritic complexity in the hippocampus, and ameliorated social and repetitive behavioral abnormalities in offspring.

These findings provide in vivo evidence that HIF-1α is a key upstream mediator linking prenatal hypoxic stress to PTEN/PI3K/AKT pathway dysregulation and subsequent neurodevelopmental impairment. Targeted modulation of HIF-1α during gestation emerges as a potential means to counteract hypoxia-related neurodevelopmental disturbances while providing mechanistic insight into environmentally driven ASD vulnerability. From a nanomedicine perspective, this work establishes a proof-of-concept framework for prenatal, target-directed modulation of disease-relevant signaling pathways using transferrin-modified lipid nanoparticles. Nevertheless, because the present study was conducted in a rodent model and safety assessment was limited primarily to neonatal survival and gross developmental observations, further studies involving optimized biodistribution analysis, comprehensive maternal-fetal toxicology, long-term neurodevelopmental follow-up, and validation in larger animal models are required before translational application can be considered.

## Abbreviations

ASD, autism spectrum disorder; HIF-1α, hypoxia-inducible factor-1α; SD, Sprague-Dawley; PTEN, phosphatase and tensin homolog deleted on chromosome ten; PI3K, phosphatidylinositol-4,5-bisphosphate 3-kinase; AKT, protein kinase B; tLNPs, transferrin modified lipid nanoparticles; E17, Embryonic day 17; tLNP, transferrin-modified blank lipid nanoparticle; tLNP/siHIF, transferrin-modified lipid nanoparticles encapsulating HIF-1α siRNA; siRNA, small interfering RNA; LNPs, lipid nanoparticles; LNP, empty lipid nanoparticle; Trf, transferrin; PDI; polydispersity index; PALS, phase analysis light scattering; EE, encapsulation efficiency; TEM, transmission electron microscopy; PVDF, polyvinylidene fluoride; HRP, horseradish peroxidase; WT, wild-type; PBS, phosphate-buffered saline; SEM, standard error of the mean; ANOVA, one-way analysis of variance.

## Data Sharing Statement

The datasets generated and/or analyzed during the current study are available from the corresponding author upon reasonable request.

## Ethics Approval and Consent to Participate

All animal experiments were approved by the Institutional Animal Care and Use Committee of Chongqing Medical University and were conducted in accordance with national guidelines for the care and use of laboratory animals.

## Acknowledgments

The authors thank the staff of the Children's Hospital of Chongqing Medical University for technical assistance and animal care support. Graphical abstract was created in BioRender. (2026) BioRender.com/a6qs2wi.

## Author Contributions

All authors made a significant contribution to the work reported, whether that is in the conception, study design, execution, acquisition of data, analysis and interpretation, or in all these areas; took part in drafting, revising or critically reviewing the article; gave final approval of the version to be published; have agreed on the journal to which the article has been submitted; and agree to be accountable for all aspects of the work.

## Funding

This work was supported by the National Natural Science Foundation of China [grant number 82272590].

## Disclosure

The authors declare that they have no competing interests.

## References

1. Hirota T, King BH. Autism spectrum disorder: a review. *JAMA*. 2023;329(2):157–168. doi:10.1001/jama.2022.23661
2. Shaw KA, Williams S, Patrick ME, et al. Prevalence and early identification of autism spectrum disorder among children aged 4 and 8 years - autism and developmental disabilities monitoring network, 16 sites, United States, 2022. *MMWR Surveill Summ*. 2025;74(2):1–22. doi:10.15585/mmwr.ss7402a1
3. Maenner MJ, Warren Z, Williams AR, et al. Prevalence and characteristics of autism spectrum disorder among children aged 8 years - autism and developmental disabilities monitoring network, 11 sites, United States, 2020. *MMWR Surveill Summ*. 2023;72(2):1–14. doi:10.15585/mmwr.ss7202a1
4. Love C, Sominsky L, O'Hely M, Berk M, Vuillermin P, Dawson SL. Prenatal environmental risk factors for autism spectrum disorder and their potential mechanisms. *BMC Med*. 2024;22(1):393. doi:10.1186/s12916-024-03617-3
5. Andrade C. Autism spectrum disorder, 1: genetic and environmental risk factors. *J Clin Psych*. 2025;86(2). doi:10.4088/JCP.25f15878
6. Preciado C, Baida M, Li Y, Li Y, Demopoulos C. Prenatal exposure to hypoxic risk conditions in autistic and neurotypical youth: associated ventricular differences, sleep disturbance, and sensory processing. *Autism Res*. 2024;17(12):2547–2557. doi:10.1002/aur.3250
7. Ou J, Dong H, Dai S, et al. Development and validation of a risk score model for predicting autism based on pre- and perinatal factors. *Front Psychiatry*. 2024;15:1291356. doi:10.3389/fpsyt.2024.1291356
8. Cai XY, Ma SY, Tang MH, et al. Atoh1 mediated disturbance of neuronal maturation by perinatal hypoxia induces cognitive deficits. *Commun Biol*. 2024;7(1):1121. doi:10.1038/s42003-024-06846-7
9. Wang W, Tang J, Zhong M, Chen J, Li T, Dai Y. HIF-1 α may play a role in late pregnancy hypoxia-induced autism-like behaviors in offspring rats. *Behav Brain Res*. 2021;411:113373. doi:10.1016/j.bbr.2021.113373
10. Yang Y, Chen J, Li T, Dai Y. PX-478 alleviated the autism spectrum disorder progression of offspring rats induced by prenatal hypoxia. *J Integr Neurosci*. 2024;23(9):165. doi:10.31083/j.jin2309165
11. Zhang J, Yao M, Xia S, Zeng F, Liu Q. Systematic and comprehensive insights into HIF-1 stabilization under normoxic conditions: implications for cellular adaptation and therapeutic strategies in cancer. *Cell Mol Biol Lett*. 2025;30(1):2. doi:10.1186/s11658-024-00682-7
12. Tang J, Yang Y, Qu P, Chen J, Li T, Dai Y. The role of HIF-1α silencing in late pregnancy hypoxia-induced autism-like behavior in rat offspring. *Brain Res*. 2025;1858:149633. doi:10.1016/j.brainres.2025.149633
13. El moukhtari SH, Garbayo E, Amundarain A, et al. Lipid nanoparticles for siRNA delivery in cancer treatment. *J Control Release*. 2023;361:130–146. doi:10.1016/j.jconrel.2023.07.054
14. Jia Y, Wang X, Li L, Li F, Zhang J, Liang XJ. Lipid nanoparticles optimized for targeting and release of nucleic acid. *Adv Mater*. 2024;36(4):e2305300. doi:10.1002/adma.202305300
15. Tse WH, Higgins S, Patel D, et al. The maternal-fetal transfer of passive immunity as a mechanism of transplacental nanoparticle drug delivery for prenatal therapies. *Biomater Sci*. 2022;10(18):5243–5253. doi:10.1039/d2bm00293k
16. Susa F, Arpicco S, Pirri CF, Limongi T. An overview on the physiopathology of the blood-brain barrier and the lipid-based nanocarriers for central nervous system delivery. *Pharmaceutics*. 2024;16(7). doi:10.3390/pharmaceutics16070849
17. Eygeris Y, Gupta M, Kim J, Sahay G. Chemistry of lipid nanoparticles for RNA delivery. *Acc Chem Res*. 2022;55(1):2–12. doi:10.1021/acs.accounts.1c00544
18. McDonald EA, Gundogan F, Olveda RM, Bartnikas TB, Kurtis JD, Friedman JF. Iron transport across the human placenta is regulated by hepcidin. *Pediatr Res*. 2022;92(2):396–402. doi:10.1038/s41390-020-01201-y
19. Johnsen KB, Burkhart A, Thomsen LB, Andresen TL, Moos T. Targeting the transferrin receptor for brain drug delivery. *Prog Neurobiol*. 2019;181:101665. doi:10.1016/j.pneurobio.2019.101665
20. Tapanainen PJ, Bang P, Muller HL, Wilson K, Rosenfeld RG. Hypoxia-induced changes in insulin-like growth factors and their binding proteins in pregnant rats. *Horm Res*. 1997;48(5):227–234. doi:10.1159/000185520
21. Cornford EM, Hyman S, Cornford ME, et al. Non-invasive gene targeting to the fetal brain after intravenous administration and transplacental transfer of plasmid DNA using PEGylated immunoliposomes. *J Drug Target*. 2016;24(1):58–67. doi:10.3109/1061186x.2015.1055569
22. Bartlett DW, Davis ME. Insights into the kinetics of siRNA-mediated gene silencing from live-cell and live-animal bioluminescent imaging. *Nucleic Acids Res*. 2006;34(1):322–333. doi:10.1093/nar/gkj439
23. Whitehead KA, Langer R, Anderson DG. Knocking down barriers: advances in siRNA delivery. *Nat Rev Drug Discov*. 2009;8(2):129–138. doi:10.1038/nrd2742
24. Huang Z, Wen Y, Shandilya R, Marks JR, Berchuck A, Murphy SK. High throughput detection of M6P/IGF2R intronic hypermethylation and LOH in ovarian cancer. *Nucleic Acids Res*. 2006;34(2):555–563. doi:10.1093/nar/gkj468
25. Zhang JW, Tabassum S, Jiang JX, Long C. Optimized Golgi-Cox staining validated in the hippocampus of spared nerve injury mouse model. *Front Neuroanat*. 2020;14:585513. doi:10.3389/fnana.2020.585513
26. Mei C, Jiang X, Gu Y, et al. YY1-mediated reticulocalbin-2 upregulation promotes the hepatocellular carcinoma progression via activating MYC signaling. *Am J Cancer Res*. 2021;11(5):2238–2251.
27. Shi J, Lv X, Zeng L, et al. CircPVT1 promotes proliferation of lung squamous cell carcinoma by binding to miR-30d/e. *J Exp Clin Cancer Res*. 2021;40(1):193. doi:10.1186/s13046-021-01976-w
28. Modabbernia A, Velthorst E, Reichenberg A. Environmental risk factors for autism: an evidence-based review of systematic reviews and meta-analyses. *Mol Autism*. 2017;8:13. doi:10.1186/s13229-017-0121-4

29. Khachadourian V, Mahjani B, Sandin S, et al. Comorbidities in autism spectrum disorder and their etiologies. *Transl Psychiatry*. 2023;13(1):71. doi:10.1038/s41398-023-02374-w
30. Yenkoyan K, Mkhitaryan M, Bjørklund G. Environmental risk factors in autism spectrum disorder: a narrative review. *Curr Med Chem*. 2024;31 (17):2345–2360. doi:10.2174/0109298673252471231121045529
31. Kolevzon A, Gross R, Reichenberg A. Prenatal and perinatal risk factors for autism: a review and integration of findings. *Arch Pediatr Adolesc Med*. 2007;161(4):326–333. doi:10.1001/archpedi.161.4.326
32. Zeidan J, Fombonne E, Scorah J, et al. Global prevalence of autism: a systematic review update. *Autism Res*. 2022;15(5):778–790. doi:10.1002/aur.2696
33. Wang Z, Zhang B, Mu C, et al. Androgen levels in autism spectrum disorders: a systematic review and meta-analysis. *Front Endocrinol*. 2024;15:1371148. doi:10.3389/fendo.2024.1371148
34. White TA, Miller SL, Sutherland AE, Allison BJ, Camm EJ. Perinatal compromise affects development, form, and function of the hippocampus part one; clinical studies. *Pediatr Res*. 2024;95(7):1698–1708. doi:10.1038/s41390-024-03105-7
35. Nichols ES, Grace M, Correa S, et al. Sex- and age-based differences in fetal and early childhood hippocampus maturation: a cross-sectional and longitudinal analysis. *Cereb Cortex*. 2024;34(1). doi:10.1093/cercor/bhad421
36. Semenza GL. Hypoxia-inducible factors in physiology and medicine. *Cell*. 2012;148(3):399–408. doi:10.1016/j.cell.2012.01.021
37. Večeřa J, Procházková J, Šumberová V, et al. Hypoxia/Hif1α prevents premature neuronal differentiation of neural stem cells through the activation of Hes1. *Stem Cell Res*. 2020;45:101770. doi:10.1016/j.scr.2020.101770
38. Li L, Candelario KM, Thomas K, et al. Hypoxia inducible factor-1α (HIF-1α) is required for neural stem cell maintenance and vascular stability in the adult mouse SVZ. *J Neurosci*. 2014;34(50):16713–16719. doi:10.1523/jneurosci.4590-13.2014
39. Penzes P, Cahill ME, Jones KA, VanLeeuwen JE, Woolfrey KM. Dendritic spine pathology in neuropsychiatric disorders. *Nat Neurosci*. 2011;14 (3):285–293. doi:10.1038/nn.2741
40. Rossidis AC, Stratigis JD, Chadwick AC, et al. In utero CRISPR-mediated therapeutic editing of metabolic genes. *Nat Med*. 2018;24 (10):1513–1518. doi:10.1038/s41591-018-0184-6
41. Ricciardi AS, Bahal R, Farrelly JS, et al. In utero nanoparticle delivery for site-specific genome editing. *Nat Commun*. 2018;9(1):2481. doi:10.1038/s41467-018-04894-2
42. Ahn NJ, Stratigis JD, Coons BE, Flake AW, Nah-Cederquist HD, Peranteau WH. Intravenous and intra-amniotic in utero transplantation in the Murine model. *J Vis Exp*. 2018;(140). doi:10.3791/58047
43. Winkler SM, Harrison MR, Messersmith PB. Biomaterials in fetal surgery. *Biomater Sci*. 2019;7(8):3092–3109. doi:10.1039/c9bm00177h
44. Nie Y, Li S, Yan T, et al. Propofol attenuates isoflurane-induced neurotoxicity and cognitive impairment in fetal and offspring mice. *Anesth Analg*. 2020;131(5):1616–1625. doi:10.1213/ane.0000000000004955
45. Parikh JM, Warner L, Chatterjee D. Anesthetic considerations for fetal interventions. *Semin Pediatr Surg*. 2024;33(5):151455. doi:10.1016/j.sempedsurg.2024.151455
46. Thomsen MS, Johnsen KB, Kucharz K, Lauritzen M, Moos T. Blood-brain barrier transport of transferrin receptor-targeted nanoparticles. *Pharmaceutics*. 2022;14(10). doi:10.3390/pharmaceutics14102237
47. Orberger G, Fuchs H, Geyer R, Gessner R, Köttgen E, Tauber R. Structural and functional stability of the mature transferrin receptor from human placenta. *Arch Biochem Biophys*. 2001;386(1):79–88. doi:10.1006/abbi.2000.2177
48. Moos T, Morgan EH. Transferrin and transferrin receptor function in brain barrier systems. *Cell Mol Neurobiol*. 2000;20(1):77–95. doi:10.1023/a:1006948027674
49. Knutson AK, Williams AL, Boisvert WA, Shohet RV. HIF in the heart: development, metabolism, ischemia, and atherosclerosis. *J Clin Invest*. 2021;131(17). doi:10.1172/jci137557
50. Chen S, Liu Y, Rong X, Li Y, Zhou J, Lu L. Neuroprotective role of the PI3 Kinase/Akt signaling pathway in Zebrafish. *Front Endocrinol*. 2017;8:21. doi:10.3389/fendo.2017.00021
51. Frazier TW, Jaini R, Busch RM, et al. Cross-level analysis of molecular and neurobehavioral function in a prospective series of patients with germline heterozygous PTEN mutations with and without autism. *Mol Autism*. 2021;12(1):5. doi:10.1186/s13229-020-00406-6
52. Frazier TW. Autism spectrum disorder associated with germline heterozygous PTEN mutations. *Cold Spring Harb Perspect Med*. 2019;9(10). doi:10.1101/cshperspect.a037002
53. Dempsey DR, Viennet T, Iwase R, et al. The structural basis of PTEN regulation by multi-site phosphorylation. *Nat Struct Mol Biol*. 2021;28 (10):858–868. doi:10.1038/s41594-021-00668-5
54. Chen L, Liu S, Tao Y. Regulating tumor suppressor genes: post-translational modifications. *Signal Transduct Target Ther*. 2020;5(1):90. doi:10.1038/s41392-020-0196-9
55. Meisner OC, Nair A, Chang SWC. Amygdala connectivity and implications for social cognition and disorders. *Handb Clin Neurol*. 2022;187:381–403. doi:10.1016/b978-0-12-823493-8.00017-1
56. Berraondo P, Martini PGV, Avila MA, Fontanellas A. Messenger RNA therapy for rare genetic metabolic diseases. *Gut*. 2019;68(7):1323–1330. doi:10.1136/gutjnl-2019-318269
57. Cheng Q, Wei T, Farbiak L, Johnson LT, Dilliard SA, Siegwart DJ. Selective organ targeting (SORT) nanoparticles for tissue-specific mRNA delivery and CRISPR-Cas gene editing. *Nat Nanotechnol*. 2020;15(4):313–320. doi:10.1038/s41565-020-0669-6
58. Fenton OS, Olafson KN, Pillai PS, Mitchell MJ, Langer R. Advances in biomaterials for drug delivery. *Adv Mater*. 2018;e1705328. doi:10.1002/adma.201705328